Circulation: Cardiovascular Imaging

INNOVATIONS IN IMAGING

Impaired Cardiac and Skeletal Muscle Energetics Following Anthracycline Therapy for Breast Cancer

David T. Gamble, MBBS; James Ross, PhD; Hilal Khan, MB BCh, BAO; Andreas Unger, PhD; Lesley Cheyne, BSc; Amelia Rudd, BSc; Fiona Saunders, PhD; Janaki Srivanasan, BSE; Sylvia Kamya, MBBS; Graham Horgan, PhD; Andrew Hannah, MD; Santosh Baliga, MBChB; Carlo Gabriele Tocchetti, PhD; Gordon Urquhart, MBChB; Wolfgang A. Linke, PhD; Yazan Masannat, MD; Ahmed Mustafa, MBBS; Mairi Fuller, MD; Beatrix Elsberger, PhD; Ravi Sharma, MD; Dana Dawson, D.Phil

BACKGROUND: Anthracycline-related cardiac toxicity is a recognized consequence of cancer therapies. We assess resting cardiac and skeletal muscle energetics and myocyte, sarcomere, and mitochondrial integrity in patients with breast cancer receiving epirubicin.

METHODS: In a prospective, mechanistic, observational, longitudinal study, we investigated chemotherapy-naive patients with breast cancer receiving epirubicin versus sex- and age-matched healthy controls. Resting energetic status of cardiac and skeletal muscle (phosphocreatine/gamma ATP and inorganic phosphate [Pi]/phosphocreatine, respectively) was assessed with ^{31}P-magnetic resonance spectroscopy. Cardiac function and tissue characterization (magnetic resonance imaging and 2D-echocardiography), cardiac biomarkers (serum NT-pro-BNP and high-sensitivity troponin I), and structural assessments of skeletal muscle biopsies were obtained. All study assessments were performed before and after chemotherapy.

RESULTS: Twenty-five female patients with breast cancer (median age, 53 years) received a mean epirubicin dose of 304 mg/m^2, and 25 age/sex-matched controls were recruited. Despite comparable baseline cardiac and skeletal muscle energetics with the healthy controls, after chemotherapy, patients with breast cancer showed a reduction in cardiac phosphocreatine/gamma ATP ratio (2.0±0.7 versus 1.1±0.5; P=0.001) and an increase in skeletal muscle Pi/phosphocreatine ratio (0.1±0.1 versus 0.2±0.1; P=0.022). This occurred in the context of increases in left ventricular end-systolic and end-diastolic volumes (P=0.009 and P=0.008, respectively), T1 and T2 mapping (P=0.001 and P=0.028, respectively) but with preserved left ventricular ejection fraction, mass and global longitudinal strain, and no change in cardiac biomarkers. There was preservation of the mitochondrial copy number in skeletal muscle biopsies but a significant increase in areas of skeletal muscle degradation (P=0.001) in patients with breast cancer following chemotherapy. Patients with breast cancer demonstrated a reduction in skeletal muscle sarcomere number from the prechemotherapy stage compared with healthy controls (P=0.013).

CONCLUSIONS: Contemporary doses of epirubicin for breast cancer treatment result in a significant reduction of cardiac and skeletal muscle high-energy ^{31}P-metabolism alongside structural skeletal muscle changes.

REGISTRATION: URL: https://www.clinicaltrials.gov; Unique identifier: NCT04467411

GRAPHIC ABSTRACT: A graphic abstract is available for this article.

Key Words: anthracycline ■ breast cancer ■ cardiac energetics ■ chemotherapy ■ skeletal muscle

Circulation: Cardiovascular Imaging is available at www.ahajournals.org/journal/circimaging

CLINICAL PERSPECTIVE

We have demonstrated impairment of high-energy phosphate metabolism in the myocardium and skeletal muscle, alongside structural changes in the skeletal muscle, in low-risk patients with breast cancer following anthracycline chemotherapy compared with healthy controls. Although their left ventricular ejection fraction was preserved and none fulfilled the current criteria for cancer-related therapy cardiac dysfunction, the significant reductions in cardiac and skeletal energetics observed here challenge the view that anthracycline-induced cardiotoxicity occurs only in a relatively small proportion of patients.

Nonstandard Abbreviations and Acronyms

γATP	γ-adenosine triphosphate
ACTN2	alpha-actinin-2
NT-pro-BNP	N-terminal pro-B-type natriuretic peptide
PCr	phosphocreatine
Pi	inorganic phosphate
TTN	titin

Anthracycline-related cardiac dysfunction is a recognized consequence of cancer therapies. Stages of cardiotoxicity have been defined based on reduction of left ventricular ejection fraction (LVEF) and global longitudinal strain, and a rise in cardiac biomarkers.[1] However, subtle myocardial changes occur much earlier than a measurable decline in the LV systolic function, demonstrated by increases in parametric (T1 and T2) myocardial mapping on cardiac magnetic resonance imaging,[2,3] which imply the presence of myocardial edema and other histopathologic abnormalities. Experimental evidence suggests that the mechanisms responsible for these abnormalities include free radical production with consequent mitochondrial dysfunction, suppression of myofilament protein synthesis, and reduction in cardiac energetics.[4,5]

Thus far, trials of cardioprotective therapies (such as angiotensin-converting enzyme inhibitors, beta-blockers, or statins) during anthracycline chemotherapy did not prevent a small but measurable reduction in left venrticular (LV) ejection fraction (EF) after extended follow-up.[6,7] For the success of primary prevention therapies, it would be important to have the ability to detect measurable end points directly related to specific pathways of myocyte derangement, such as mitochondria-related cardiac energetics. A decrease in cardiac energetics has been shown to precede the subsequent onset of LV dysfunction in vivo in animal models of anthracycline-induced cardiomyopathy,[4] but it remains unknown if this is found in human patients receiving standard chemotherapy doses. Furthermore, despite the systemic toxicity profile of anthracyclines, their effects on skeletal muscle myocytes in humans are significantly under-investigated. Questions remain as to whether energetic or structural changes also occur in skeletal muscle, to indicate skeletal muscle stress.[8] This is important as physical exercise training during chemotherapy has been proposed as a primary prevention strategy for functional disability.[9] In this study, we assess resting cardiac and skeletal muscle energetics in patients with breast cancer undergoing anthracycline-based chemotherapy. Using skeletal muscle biopsies, we simultaneously investigate basic sarcomere and mitochondrial integrity to distinguish between functional and structural causes of anthracycline-induced toxicity.

METHODS

Upon reasonable request, the authors will make the data, methods used in the analysis, and materials used to conduct the research available to any researcher for purposes of reproducing the results or replicating the procedure, as long as this does not compromise patient confidentiality, within 1 year of publication.

Study Design

This was a prospective, mechanistic, observational, longitudinal investigation enrolling a cohort of anthracycline-naive female patients with breast cancer at Aberdeen Royal Infirmary between 2021 and 2022. Patients were enrolled if they were scheduled for adjuvant or neo-adjuvant anthracycline-based chemotherapy regimen as 3 cycles of 5-fluorouracil, epirubicin, and cyclophosphamide followed by 3 cycles of docetaxel. Patients were studied at 2 time points: at baseline before the first cycle of chemotherapy and a final examination taking place within 6 weeks of their last cycle of chemotherapy but before any radiotherapy-based treatment. A group of healthy control women was recruited for comparison and studied at a single time point. Study assessments included cardiac and skeletal muscle [31]Phosphorus-spectroscopy, cardiac magnetic resonance, transthoracic echocardiography, blood sampling, and skeletal muscle biopsy. The study was approved by the Institutional Review Board (North of Scotland Ethics Committee One), and all participants provided informed consent. Two participants did not return for follow-up.

Full investigative protocols and analyses of all methodology described below are presented in the Supplemental Material. A flow diagram of recruitment and study numbers is shown in Figure S1.

[31]P-Magnetic Resonance Cardiac and Skeletal Muscle Spectroscopy Acquisition and Analysis

All participants were scanned on a 3T Philips scanner (Achieva, Philips Medical Systems, Best, the Netherlands). [31]P- Magnetic

Resonance Spectroscopy was acquired using a 14-cm diameter transmit/receive ^{31}P surface coil (Philips Healthcare, Best, the Netherlands).[10] Skeletal muscle ^{31}P-spectrsocopy was performed using the same coil placed over the vastus lateralis muscle. For in vivo resting cardiac energetics, the phosphocreatine/γ-ATP (γATP) ratio was determined after the γATP was corrected for blood contamination and saturation correction applied as described previously.[11] For skeletal muscle (vastus lateralis) resting energetics, the inorganic phosphate (Pi)/phosphocreatine ratio was derived.

Cardiac Magnetic Resonance Imaging Acquisition and Analysis

A 5-channel phased array surface coil was used to acquire an ECG-gated cardiac magnetic resonance protocol inclusive of cine imaging, T1/T2 mapping, and late gadolinium enhancement. Cardiac magnetic resonance images were analyzed in Circle cvi42 v5.16 (Circle Cardiovascular Imaging, Calgary, Canada) for deriving indexed LV volumes and mass, and EF. T1 and T2 maps were analyzed with the Philips IntelliSpace software Version 11.1 (Koninklijke Philips N.V., Amsterdam, the Netherlands). The myocardial extracellular volume fraction was calculated for the whole left ventricle. Analysis of all cardiac magnetic resonance and spectroscopy was performed on anonymized data at the end of the study and blinded to the pre/post-chemotherapy status of the participants.

Two-Dimensional Transthoracic Echocardiography and Image Analysis

Two-dimensional and Doppler Echocardiography was performed using a Vivid E9 system with a 2.5-MHz (M5S) transducer (GE Vingmed, Horten, Norway) by a British Society of Echocardiography-accredited sonographer and image analysis performed by 2 experienced operators (D.T.G. and J.S.) on the TOMTEC-ARENA v6 (Tomtec, Unterschleissheim, Germany).

Cardiovascular Biomarkers

NT-pro-BNP (N-terminal pro-B-type natriuretic peptide) and high-sensitivity troponin I were analyzed using an Abbott Alinity I Immunoassay System Analyser (Abbott, IL).

Skeletal Muscle Biopsies

Skeletal muscle biopsies (10 mg) from the left vastus lateralis were obtained with a Bard Magnum disposable core tissue biopsy needle (Bard Medical, Covington, GA) using an aseptic technique, immediately snap-frozen in liquid nitrogen and placed in dry storage at −80 °C until analysis.

Real-Time Quantitative PCR

Real-time quantitative polymerase chain reaction was performed to determine mitochondrial DNA copy number. Samples were analyzed on a Roche LightCycler 480 II (F. Hoffmann-La Roche AG, Basel, Switzerland) using LightCycler 480 (v1.5.1.62 SP3) software. Data were expressed as mitochondrial copy number per 10 ng of RNA.

Transmission Electron Microscopy and Immunofluorescence Confocal Laser Microscopy

Transmission electron microscopy was processed as described.[12] Areas that demonstrated breakdown of the normal cytoplasmic organelles and sarcomeric apparatus were measured from electron micrographs and demarcated as areas of degradation as previously described.[13,14] These were calculated as percentage degradation of full skeletal muscle areas (each biopsy, 225 000 μm²).

Confocal laser microscopy imaging for quantitation of sarcomere loss was done as previously described.[15] The number of striation signals (sarcomere bands) within a 100-μm² cell area was calculated on immunofluorescent images labeled with primary antibody TTN-Z (titin). One Z-disc signal was counted as 1 sarcomere. A total of 400 to 800 antibody-marked striation signals were counted per sample. To allow for intersample comparison, we measured the immunofluorescent signals at a sarcomere length of minimum of 1.8 μm.

Statistical Analysis

Statistical analysis was performed using IBM SPSS statistics Version 28.0. Descriptive statistics were presented as mean±SD or number (%), unless stated otherwise. To detect a change from baseline to post-chemotherapy follow-up in patients with breast cancer of 0.5 (SD difference, 0.6) for the primary end point of phosphocreatine/γATP ratio, with β=0.8, and a 2-sided significance level of 0.05, the sample size required 12 participants for paired follow-up. Comparisons between healthy volunteers and patients with breast cancer were made using ANOVA for all response variables and logistic regression for binary categorical measures. Body mass index was included as a covariate in the ANOVA and logistic regression analysis. Comparisons between patients with breast cancer at baseline and after chemotherapy were made using paired samples t tests. A mixed linear model was used for all other data with study visits as a fixed effect and the unique participant identifier as a random effect. Statistical significance was set at $P<0.05$.

RESULTS

Twenty-five female patients with breast cancer and 25 age/sex-matched controls were recruited. Participants' baseline characteristics are presented in Table 1. The median age of the breast cancer group was 53 years (range, 32–74 years), they had a mean body mass index of 30 kg/m² and minimal cardiovascular comorbidities with only 2 (8%) participants receiving renin-angiotensin inhibitor treatment for hypertension. All patients with breast cancer received 5-fluorouracil, epirubicin, cyclophosphamide, and docetaxel as their chemotherapy regimen with a cumulative epirubicin dose of 304±20 mg/m². Three participants (12%) also received trastuzumab. The median follow-up time from the first date of chemotherapy to their final study visit was 145 days (range, 123–265 days). The healthy volunteer group

Table 1. Controls and Breast Cancer Participants Clinical Characteristics, Pathology, and Treatment

	Healthy volunteers (n=25)	Patients with breast cancer (n=25)	P value
Age, y; median (range)	51 (23–71)	53 (32–74)	0.141
Body mass index	26.4±4.1	29.7±6.7	0.045
Current/ex smoker	4 (14)	8 (24)	0.185
Framingham risk score for 10-y risk of MI or death, (%)	1.4±1.1	3.7±2.7	0.119
Follow-up time, d; median (range)	…	145 (123–265)	…
Comorbidities			
Hypertension	0 (0)	2 (8)	0.149
Ischemic heart disease	0 (0)	0 (0)	…
Diabetes	0 (0)	0 (0)	…
Atrial fibrillation or flutter	0 (0)	0 (0)	…
Hypercholesterolemia	0 (0)	0 (0)	…
Medication			
Angiotensin-converting enzyme inhibitors	0 (0)	2 (8)	0.149
Beta blocker	0 (0)	0 (0)	…
Antiplatelets/anticoagulants	0 (0)	0 (0)	…
Statin	0 (0)	0 (0)	…
Hematology and biochemistry			
Hemoglobin g/L	140.0±6.6	138.4±8.4	0.607
Hematocrit L/L	0.4±0.02	0.4±0.02	0.883
eGFR mL/min per m²	>60	>60	0.540
Cholesterol mmol/L	5.6±0.8	6.1±0.9	0.150
C-reactive protein mg/L	2.0±1.3	4.6±3.5	0.008
Breast cancer location			
Right sided	…	9 (36)	…
Left sided	…	15 (60)	…
Bilateral	…	1 (4)	…
Oncological treatment regimen and dose			
Chemotherapy duration, d; median (range)	…	112 (105–232)	
Adjuvant	…	23 (92)	…
Neo-adjuvant	…	2 (8)	…
FEC-T	…	25 (100)	…
Mean cumulative epirubicin dose, mg/m²	…	304.2±20.4	…
Aromatase inhibitors	…	13 (52)	…
Bisphosphonates	…	18 (72)	…
Goserelin	…	7 (28)	…
Trastuzumab	…	3 (12)	…

Data shown as mean±SD or number (%), unless stated otherwise. eGFR indicates estimated glomerular filtration rate; FEC-T, fluorouracil (5FU), epirubicin, cyclophosphamide, docetaxel; and MI, myocardial infarction.

had a median age of 51 years (range, 23–71 years), a mean body mass index of 26 kg/m², and were free of any health conditions.

Cardiac Energetics, Cardiac Magnetic Resonance Imaging, 2D-Echocardiography, and Cardiac Biomarkers

There was no difference in the myocardial corrected phosphocreatine/γATP ratio nor the indexed LV end-diastolic or end-systolic volumes, indexed LV mass, cardiac magnetic resonance imaging, or echocardiography-derived LVEF, T1 mapping, T2 mapping or global longitudinal strain between the healthy volunteers and the patients with breast cancer before chemotherapy—Table 2.

However, following chemotherapy, patients with breast cancer had a significant reduction in the myocardial corrected phosphocreatine/γATP ratio compared with their own baseline at prechemotherapy assessment (1.1±0.5 versus 2.0±0.7; P=0.001)—Table 2 and Figure 1. This was accompanied by increases in indexed LV end-diastolic (P=0.008) and end-systolic (P=0.009) volumes, as well as LV native T1 (P=0.001) and T2 (P=0.028) mapping in the patients with breast cancer after chemotherapy compared with their baseline. Conversely, their LVEF, indexed LV mass, extracellular volume fraction, and echocardiography-derived global longitudinal strain remained unchanged post-chemotherapy—Table 2. Therefore, at the point of follow-up, no participants developed chemotherapy-related cardiotoxicity as defined in the European Society of Cardiology guidelines.[16] There was no late gadolinium enhancement in patients with breast cancer before, or after chemotherapy. There was no correlation between LVEF and phosphocreatine/γATP ratio at follow-up (P=0.721). There was no significant difference in NT-pro-BNP (P=0.076) or high-sensitivity troponin I (P=0.835) in patients with breast cancer after chemotherapy compared with prechemotherapy or healthy controls.

Skeletal Muscle Energetics and Structural Integrity

There was no significant difference in the Pi/phosphocreatine ratio between healthy volunteers and patients with breast cancer at prechemotherapy stage (P=0.890). However, there was a significant increase in Pi/phosphocreatine ratio measured in breast cancer patients' post-chemotherapy (0.22±0.14 versus 0.13±0.05; P=0.022)—Table 3 and Figure 1.

There was no significant difference in skeletal muscle pH ratio between healthy volunteers and patients with breast cancer at baseline (P=0.116) or between patients with breast cancer at baseline and at follow-up (P=0.758). Real-time quantitative phosphocreatine showed comparable copy number of mitochondria in healthy volunteers and

Table 2. Cardiac Energetics, Cardiac Magnetic Resonance Imaging, 2D-Echocardiography, and Serum Cardiac Biomarkers

	Healthy controls	Baseline prechemotherapy patients with breast cancer	P value healthy controls vs patients with breast cancer at baseline	Following chemotherapy patients with breast cancer	P value patients with breast cancer at baseline vs at follow-up
Cardiac ³¹P-magnetic resonance spectroscopy (n=15 per group)					
PCr/γATP ratio	2.3±0.6	2.0±0.7	0.513	1.1±0.5	0.001
Cardiac magnetic resonance (n=22 per group)					
Indexed LV end diastolic volume, mL/m²	62.4±13.5	64.7±9.8	0.546	70.2±13.4	0.009
Indexed LV systolic volume, mL/m²	20.1±5.0	22.6±5.0	0.136	26.1±6.7	0.008
Indexed LV mass, g/m²	60.6±5.5	56.3±8.6	0.159	52.7±6.3	0.111
Ejection fraction	68.1±5.2	65.5±4.7	0.107	63.3±5.6	0.140
T1 left ventricle, ms	1274.2±22.9	1289.1±29.2	0.118	1317.9±29.4	0.001
T2 left ventricle, ms	48.0±1.8	50.4±3.8	0.110	54.0±6.3	0.028
Extracellular volume fraction left ventricle	…	0.28±0.02	…	0.31±0.03	0.078
Echocardiography (n=25 per group)					
Ejection fraction	65.7±4.1	65.9±6.1	0.757	63.2±5.0	0.155
Global longitudinal strain	−19.8±1.6	−22.7±3.9	0.086	−20.8±4.8	0.200
Cardiac biomarkers (n=25 per group)					
N-terminal pro-B-type natriuretic peptide, pg/mL	60.2±21.5	49.0±24.9	0.211	88.5±76.0	0.076
High-sensitivity troponin I, ng/L	3.6±6.2	3.7±6.5	0.970	6.4±11.3	0.835

Data shown as mean±SD. γATP indicates gamma ATP; LV, left ventricular; and PCr, phosphocreatine.

prechemotherapy breast cancer patients (P=0.730). There was no loss in the number of mitochondria of skeletal muscle cells in post-chemotherapy breast cancer patients (P=0.590) (Table 3). Transmission electron microscopy did not show any difference in the measured area of skeletal muscle degradation between the healthy volunteers and prechemotherapy breast cancer patients (P=0.203). However, there was a significant increase in skeletal muscle degradation in the patients with breast cancer post- compared with prechemotherapy compared with baseline (P=0.001)—Table 3 and Figure 2. Immunofluorescent confocal microscopy showed a significant reduction in sarcomere count per unit area (S/A [µm²]) in patients with breast cancer compared with controls (P=0.013). There was no difference in sarcomere number in the patients with breast cancer before and after chemotherapy (P=0.112)—Table 3 and Figure 3. The observed cardiac and skeletal muscle findings remained unchanged when those participants who also received Trastuzumab (n=3) were removed from the analysis, inclusive of the primary end point of cardiac phosphocreatine/yATP ratio (1.9±0.5 versus 1.2±0.5; P=0.004). There was no association between participants' body mass index and the impairments of high-energy phosphate metabolism in cardiac (P=0.478) and skeletal muscle (P=0.729).

DISCUSSION

In this prospective study, we report significant reductions in resting cardiac and skeletal muscle energetics in patients with breast cancer after administration of standard clinical doses of anthracycline chemotherapy. There was preservation of the number of skeletal muscle mitochondria but increased skeletal muscle degradation after epirubicin-containing chemotherapy. Patients with breast cancer had reduced numbers of sarcomeres compared with healthy controls from prechemotherapy stage.

This is the first human study to demonstrate impairment of LV high-energy phosphate metabolism in patients with breast cancer following administration of contemporary doses of anthracyclines. Our center uses epirubicin, an anthracycline with a lesser cardiotoxic profile compared with the more widely used doxorubicin.[17] The studied patient cohort had a very low cardiovascular risk profile; thus, we are confident that we have evaluated the effect of chemotherapy on myocardial energetics without the confounding contribution of other comorbidities. Despite their low cardiovascular risk profile, small increases in indexed LV volumes and parametric mapping were detected, in keeping with several previous reports.[18] However, at this stage of follow-up, we did not observe a reduction in the LVEF nor LV mass, both of which may have been adversely
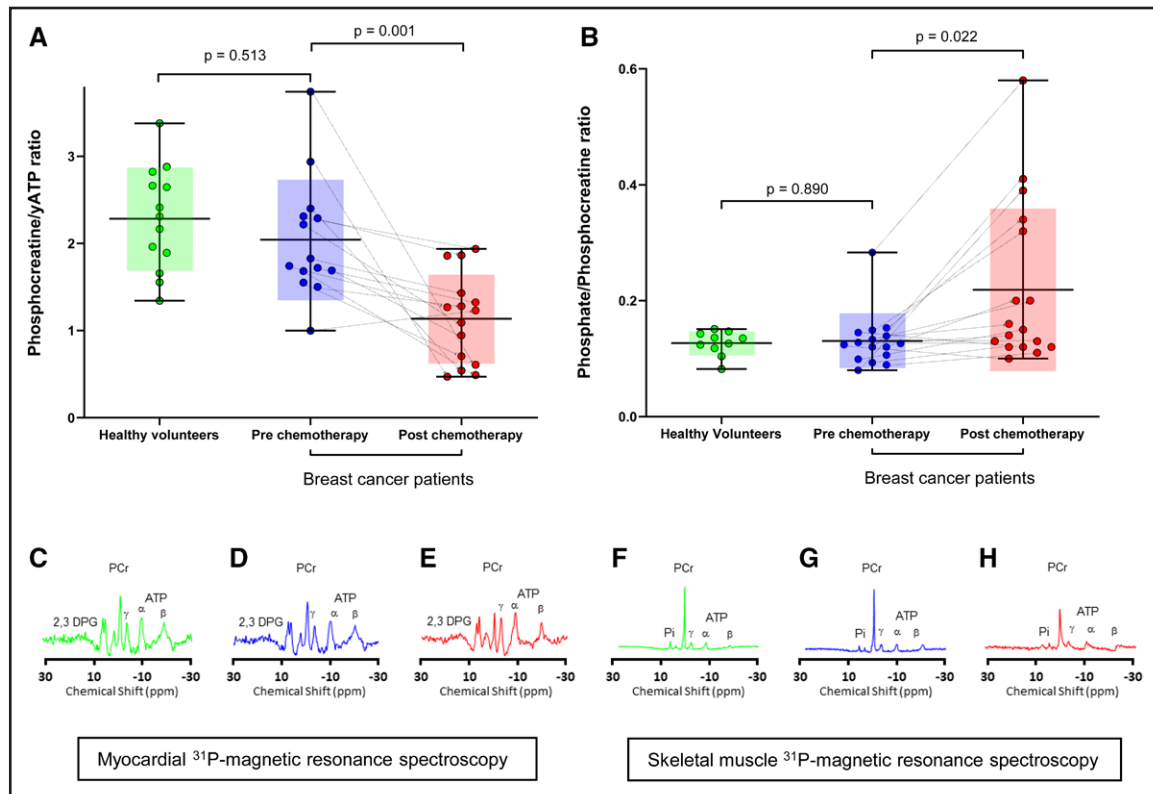
Figure 1. ^{31}P-magnetic resonance spectroscopy for cardiac and skeletal muscle energetics.
Data shown as box plots/error bars and superimposed individual, paired data points with mean line, box for SDs and error bars for minimum and maximum. **A**, Corrected phosphocreatine (PCr)/gamma ATP (γATP) in the myocardium and (**B**) inorganic phosphate (Pi)/PCr in the skeletal muscle, for healthy controls and patients with breast cancer before chemotherapy and after chemotherapy. Below are example spectra showing PCr, γ, β, and α ATP, and 2,3-diphosphoglycerate (2,3 DPG) peaks in healthy volunteers (**C**) and in paired patients with breast cancer before (**D**) and after (**E**) chemotherapy; Pi, PCr and γ, β, and α ATP peaks in healthy volunteers (**F**) and in paired patients with breast cancer before (**G**) and after (**H**) chemotherapy.

affected by more prevalent comorbidities in previously reported patients.[19,20] It is known from experimental animal models that increase in myocardial T1/T2 mapping reflective of myocardial edema, intracytoplasmic vacuolization, and myofibril loss are detectable as early as 6 weeks.[21,22] After chemotherapy, our patients with breast cancer also showed increases in T1/T2 mapping but having not done multiple points-serial assessments, we were not able to assess the relative time points of resting cardiac energetics decline versus increased parametric mapping during chemotherapy. The main purpose of our investigation was to detect if resting myocardial energetics is adversely affected in human patients, which we herewith confirmed. Importantly, this was detected in the absence of a decline in LVEF or loss of myocardial mass or increase of cardiac biomarkers. In a recent prospective study, obesity was associated (odds ratio, 3.02 [95% CI, 1.10–8.25]; P=0.03) with an important increase in risk-related cardiotoxicity[23]; however, in our study, there was no association between participants' body mass index and the impairments of high-energy phosphate metabolism in cardiac and skeletal muscle. In a recent meta-analysis, most studies demonstrated

a reduction in LVEF following doxorubicin therapy.[24] However, in our study, no participants developed chemotherapy-related cardiotoxicity as defined in the European Society of Cardiology guidelines,[16] at the point of follow-up. This reinforces prior evidence that epirubicin may be less cardiotoxic. The heart is a known omnivore, able to generate energy from glycolysis, fatty acid oxidation, as well as, other substrates such as ketone bodies[25] or branched-chain amino-acids,[26] to meet the high-energy requirements of 6 kg ATP per day. Therefore, the demonstration of energetics impairment opens new avenues of exploring cardioprotection, for example, with metabolic modulators[27] or medications that preferentially change metabolic substrate availability.[28] It has been demonstrated that empagliflozin improves cardiac remodeling and heart failure in animal models leading to a switch in myocardial fuel utilization away from glucose with consequent improvement in myocardial energetics and LV systolic function.[29] These findings suggest that targeting mitochondrial energetics directly may represent a new avenue for chemotherapy-induced cardiotoxicity therapeutics. While anthracycline-based chemotherapy is well known to negatively impact cardiac

Table 3. Skeletal Muscle Energetics and Structural Integrity

	Healthy controls	Baseline prechemotherapy patients with breast cancer	*P* value healthy controls vs patients with breast cancer at baseline	Following chemotherapy patients with breast cancer	*P* value patients with breast cancer at baseline vs at follow-up
Skeletal muscle ^{31}P-magnetic resonance spectroscopy (n=17 per group)					
Pi/PCr ratio	0.13±0.02	0.13±0.05	0.890	0.22±0.14	0.022
pH	7.03±0.01	7.05±0.04	0.116	7.05±0.1	0.758
Skeletal muscle mitochondrial copy number (n=5 per group)					
Mitochondrial copy number/10 ng RNA	$3.7×10^5±2.44×10^5$	$3.2×10^5±2.1×10^5$	0.730	$3.8×10^5±1.4×10^5$	0.590
Skeletal muscle degradation (n=3 per group)					
Area of skeletal muscle degradation	2.7±1.0	4.4±1.7	0.203	23.5±2.6	0.001
Skeletal muscle sarcomere number (n=3 per group)					
Sarcomere number (S/A [µm²])	0.5±0.01	0.4±0.05	0.013	0.3±0.002	0.112

Data shown as mean±SD. n indicates number of subjects; PCr, phosphocreatine; Pi, inorganic phosphate; and S/A, surface area.

function, the impact on skeletal muscle has received much less attention. Our findings substantiate those demonstrated in a recent prospective cohort study in patients with breast cancer treated with anthracycline chemotherapy, which also showed an increase in pi/phosphocreatine ratio in patients after chemotherapy, both at rest and after incremental intensity workloads.[30] Increasing pi/phosphocreatine ratio reflects greater ADP accumulation which triggers increased phosphocreatine breakdown to compensate for inadequate ATP production.[31] Our data show that the number of skeletal muscle mitochondria was comparable between cancer patients and healthy controls, both before and after chemotherapy. The observation that mitochondrial number was not reduced in our study suggests that the energetic impairment is related to the function of mitochondria not their overall number at this early stage. We also noted other significant perturbations of muscle homeostasis. First, cancer patients had reduced skeletal muscle sarcomere number, suggesting that the well-known associated sarcopenic process previously described in late cancer stages[32,33] might in fact commence much earlier than previously appreciated. Such reductions in skeletal muscle sarcomere number have
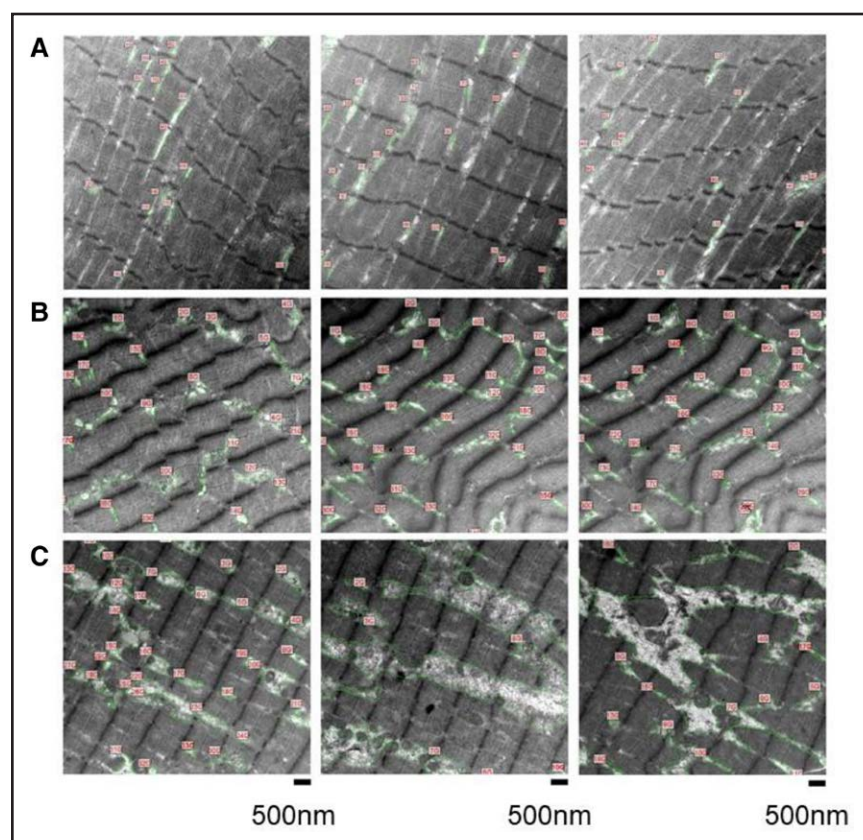

Figure 2. Transmission electron microscopy of skeletal muscle showing demarcated (green contours) areas of degradation.
Examples from (**A**) healthy volunteers, (**B**) patients with breast cancer at baseline, and (**C**) patients with breast cancer following anthracycline chemotherapy.
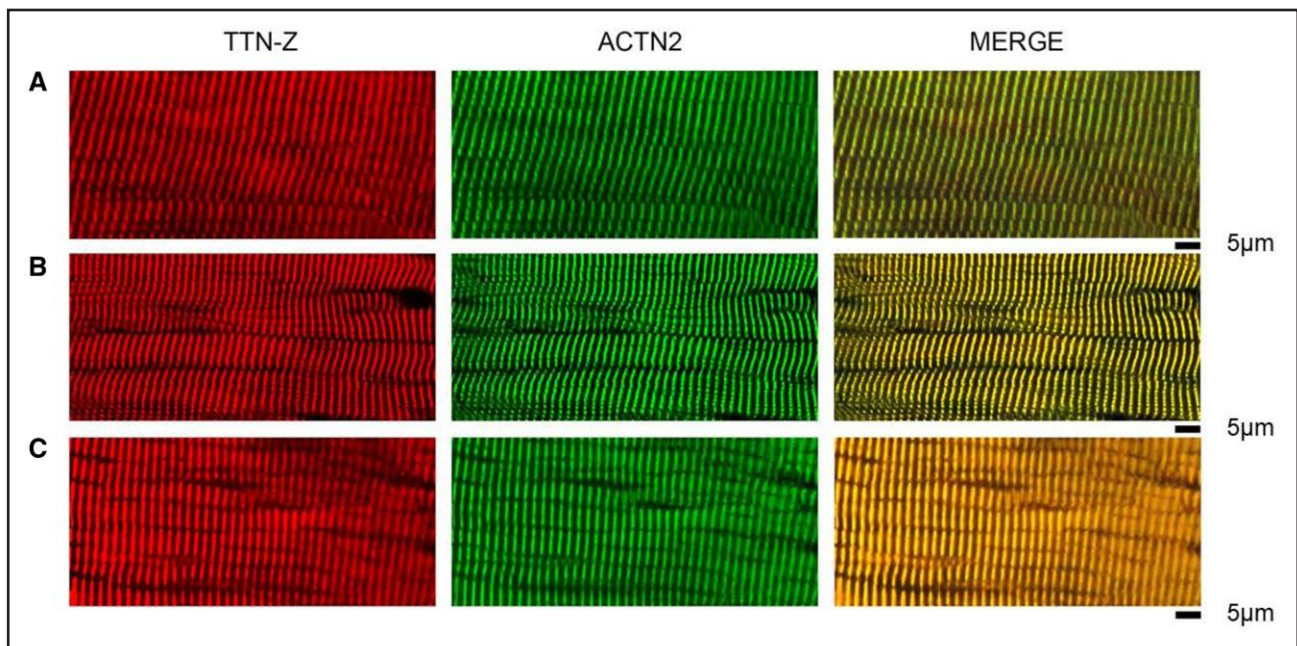
Figure 3. Confocal laser scanning microscopy analysis of skeletal muscle.
Immunofluorescence staining was done against TTN-Z (titin; red) and ACTN2 (alpha-actinin-2; green) epitopes and merged (Z-disc); examples from (**A**) healthy volunteers, (**B**) patients with breast cancer at baseline, and (**C**) patients with breast cancer following anthracycline chemotherapy.

been documented in under-stretch conditions including chronic immobilization, this change in the number of contractile units leads to reduced active force generation within muscle fibers.[34] To our knowledge, this is the first time such findings have been reported and it may represent a systemic feature of cancer. The skeletal muscle sarcomere number in our study was not negatively affected by chemotherapy administration, although we acknowledge the sample size may have been too small to conclude on this. Second, we observed an increase in areas of muscle degradation on electron microscopy after chemotherapy administration. These likely represent disrupted cytoplasmic organelles representing muscle breakdown, which are usually the precursors of fatty infiltration and muscle fibrosis.[35,36] These add further to the knowledge of anthracycline-based chemotherapy being causative in the loss of skeletal muscle mass resulting in sarcopenia[37] and impaired contractile function.[38] These degradation areas show a transition of muscle cells into lipomatous tissue and granular-filamentous aggregates seen in primary myopathies or myopathies secondary to chronic systemic conditions.[39] Future studies should focus on correlating skeletal muscle degradation with functional assessments, to further explore their impact on functional capacity. These findings of structural changes and impaired energetics within the skeletal muscle may provide explanation for the high prevalence of fatigue and functional disability[40] in these patients. These have direct clinical relevance as exercise rehabilitation during active chemotherapy is part of the current guidelines and recommendations and within the patients' anticipated expectations.[9] Perhaps unsurprisingly, the early results from randomized controlled studies of exercise training in patients with breast cancer showed that despite an increased peak oxygen consumption derived from training, functional disability was not attenuated.[41] Further work is needed to address primary prevention of cardiac and skeletal muscle dysfunction resulting from cancer therapies.

Limitations

This was a single-center study with a relatively small sample size of low cardiac risk patients with breast cancer. Our findings are confined to the chemotherapy regimens applied within this study. Due to the predominance of White women with breast cancer in our catchment area, our results may not be applicable to other ethnicities or higher risk patients, or those with a different malignancy or clinical profile. The relatively small number of skeletal muscle biopsy assessment in this study is a limitation and future studies in larger numbers should be conducted to confirm these findings.

Conclusions

We demonstrate the impairment of high-energy phosphate metabolism in the myocardium and skeletal muscle of patients with breast cancer following anthracycline chemotherapy. We also demonstrated structural changes in the skeletal muscle both predating and after

chemotherapy in cancer patients compared with healthy controls.

REFERENCES

1. Herrmann J, Lenihan D, Armenian S, Barac A, Blaes A, Cardinale D, Carver J, Dent S, Ky B, Lyon AR, et al. Defining cardiovascular toxicities of cancer therapies: an International Cardio-Oncology Society (IC-OS) consensus statement. *Eur Heart J.* 2022;43:280–299. doi: 10.1093/eurheartj/ehab674

2. Jordan JH, D'Agostino RB, Jr, Hamilton CA, Vasu S, Hall ME, Kitzman DW, Thohan V, Lawrence JA, Ellis LR, et al. Longitudinal assessment of concurrent changes in left ventricular ejection fraction and left ventricular myocardial tissue characteristics after administration of cardiotoxic chemotherapies using T1-weighted and T2-weighted cardiovascular magnetic resonance. *Circ Cardiovasc Imaging.* 2014;7:872–879. doi: 10.1161/CIRCIMAGING.114.002217

3. Lustberg MB, Reinbolt R, Addison D, Ruppert AS, Moore S, Carothers S, Suresh A, Das H, Berger M, Ramaswamy B, et al. Early detection of anthracycline-induced cardiotoxicity in breast cancer survivors with T2 cardiac magnetic resonance. *Circ Cardiovasc Imaging.* 2019;12:e008777. doi: 10.1161/CIRCIMAGING.118.008777

4. Maslov MY, Chacko VP, Hirsch GA, Akki A, Leppo MK, Steenbergen C, Weiss RG. Reduced in vivo high-energy phosphates precede adriamycin-induced cardiac dysfunction. *Am J Physiol Heart Circ Physiol.* 2010;299:H332–H337. doi: 10.1152/ajpheart.00727.2009

5. Menna P, Salvatorelli E, Minotti G. Anthracycline degradation in cardiomyocytes: a journey to oxidative survival. *Chem Res Toxicol.* 2010;23:6–10. doi: 10.1021/tx9003424

6. Heck SL, Mecinaj A, Ree AH, Hoffmann P, Schulz-Menger J, Fagerland MW, Gravdehaug B, Rosjo H, Steine K, Geisler J, et al. Prevention of cardiac dysfunction during adjuvant breast cancer therapy (PRADA): extended follow-up of a 2x2 factorial, randomized, placebo-controlled, double-blind clinical trial of candesartan and metoprolol. *Circulation.* 2021;143:2431–2440. doi: 10.1161/CIRCULATIONAHA.121.054698

7. Thavendiranathan P, Houbois C, Marwick TH, Kei T, Saha S, Runeckles K, Huang F, Shalmon T, Thorpe KE, Pezo RC, et al. Statins to prevent early cardiac dysfunction in cancer patients at increased cardiotoxicity risk receiving anthracyclines. *Eur Heart J Cardiovasc Pharmacother.* 2023;0:1–11. doi: 10.1093/ehjcvp/pvad031

8. Volkova M, Russell R 3rd. Anthracycline cardiotoxicity: prevalence, pathogenesis and treatment. *Curr Cardiol Rev.* 2011;7:214–220. doi: 10.2174/157340311799960645

9. Gilchrist SC, Barac A, Ades PA, Alfano CM, Franklin BA, Jones LW, La Gerche A, Ligibel JA, Lopez G, Madan K, et al; American Heart Association Exercise, Cardiac Rehabilitation, and Secondary Prevention Committee of the Council on Clinical Cardiology; Council on Cardiovascular and Stroke Nursing; and Council on Peripheral Vascular Disease. Cardio-oncology rehabilitation to manage cardiovascular outcomes in cancer patients and survivors: a scientific statement from the American Heart Association. *Circulation.* 2019;139:e997–e1012. doi: 10.1161/CIR.0000000000000679

10. Dawson DK, Neil CJ, Henning A, Cameron D, Jagpal B, Bruce M, Horowitz J, Frenneaux MP. Tako-tsubo cardiomyopathy: a heart stressed out of energy? *JACC Cardiovasc Imaging.* 2015;8:985–987. doi: 10.1016/j.jcmg.2014.10.004

11. Shivu GN, Abozguia K, Phan TT, Ahmed I, Henning A, Frenneaux M. (31) P magnetic resonance spectroscopy to measure in vivo cardiac energetics in normal myocardium and hypertrophic cardiomyopathy: experiences at 3T. *Eur J Radiol.* 2010;73:255–259. doi: 10.1016/j.ejrad.2008.10.018

12. Unger A, Beckendorf L, Böhme P, Kley R, von Frieling-Salewsky M, Lochmüller H, Schröder R, Fürst DO, Vorgerd M, Linke WA. Translocation of molecular chaperones to the titin springs is common in skeletal myopathy patients and affects sarcomere function. *Acta Neuropathol Commun.* 2017;5:72–70. doi: 10.1186/s40478-017-0474-0

13. Swist S, Unger A, Li Y, Vöge A, von Frieling-Salewsky M, Skärlén A, Cacciani N, Braun T, Larsson L, Linke WA. Maintenance of sarcomeric integrity in adult muscle cells crucially depends on Z-disc anchored titin. *Nat Commun.* 2020;11:4479–4472. doi: 10.1038/s41467-020-18131-2

14. Fomin A, Gärtner A, Cyganek L, Tiburcy M, Tuleta I, Wellers L, Folsche L, Hobbach AJ, von Frieling-Salewsky M, Unger A, et al. Truncated titin proteins and titin haploinsufficiency are targets for functional recovery in human cardiomyopathy due to TTN mutations. *Sci Transl Med.* 2021;13:eabd3079. doi: 10.1126/scitranslmed.abd3079

15. Fomin A, Gärtner A, Cyganek L, Tiburcy M, Tuleta I, Wellers L, Folsche L, Hobbach AJ, von Frieling-Salewsky M, Unger A, et al. Truncated titin proteins and titin haploinsufficiency are targets for functional recovery in human cardiomyopathy due to TTN mutations. *Sci Transl Med.* 2021;13:eabd3079. doi: 10.1126/scitranslmed.abd3079

16. Lyon AR, Lopez-Fernandez T, Couch LS, Asteggiano R, Aznar MC, Bergler-Klein J, Boriani G, Cardinale D, Cordoba R, Cosyns B, et al; ESC Scientific Document Group. 2022 ESC Guidelines on cardio-oncology developed in collaboration with the European Hematology Association (EHA), the European Society for Therapeutic Radiology and Oncology (ESTRO) and the International Cardio-Oncology Society (IC-OS). *Eur Heart J Cardiovasc Imaging.* 2022;43:4229–4361. doi: 10.1093/eurheartj/ehac244

17. Jain KK, Casper ES, Geller NL, Hakes TB, Kaufman RJ, Currie V, Schwartz W, Cassidy C, Petroni GR, Young CW. A prospective randomized comparison of epirubicin and doxorubicin in patients with advanced breast cancer. *J Clin Oncol.* 1985;3:818–826. doi: 10.1200/JCO.1985.3.6.818

18. Jordan JH, D'Agostino RBJ, Hamilton CA, Vasu S, Hall ME, Kitzman DW, Thohan V, Lawrence JA, Ellis LR, Lash TL, et al. Longitudinal assessment of concurrent changes in left ventricular ejection fraction and left ventricular myocardial tissue characteristics after administration of cardiotoxic chemotherapies using T1-weighted and T2-weighted cardiovascular magnetic resonance. *Circ Cardiovasc Imaging.* 2014;7:872–879. doi: 10.1161/CIRCIMAGING.114.002217

19. Jordan JH, Castellino SM, Meléndez GC, Klepin HD, Ellis LR, Lamar Z, Vasu S, Kitzman DW, Ntim WO, Brubaker PH, et al. Left ventricular mass change

after anthracycline chemotherapy. *Circ Heart Fail.* 2018;11:e004560. doi: 10.1161/CIRCHEARTFAILURE.117.004560

20. Ferreira de Souza T, Quinaglia A C Silva T, Osorio Costa F, Shah R, Neilan TG, Velloso L, Nadruz W, Brenelli F, Sposito AC, Matos-Souza JR, et al. Anthracycline therapy is associated with cardiomyocyte atrophy and preclinical manifestations of heart disease. *JACC Cardiovasc Imaging.* 2018;11:1045–1055. doi: 10.1016/j.jcmg.2018.05.012

21. Hong YJ, Park HS, Park JK, Han K, Park CH, Kim TK, Yoo SJ, Lee JY, Kim PK, Hur J, et al. Early detection and serial monitoring of anthracycline-induced cardiotoxicity using T1-mapping cardiac magnetic resonance imaging: an animal study. *Sci Rep.* 2017;7:2663. doi: 10.1038/s41598-017-02627-x

22. Galán-Arriola C, Lobo M, Vílchez-Tschischke JP, López GJ, de Molina-Iracheta A, Pérez-Martínez C, Agüero J, Fernández-Jiménez R, Martín-García A, Oliver E, et al. Serial magnetic resonance imaging to identify early stages of anthracycline-induced cardiotoxicity. *J Am Coll Cardiol.* 2019;73:779–791. doi: 10.1016/j.jacc.2018.11.046

23. Kaboré EG, Guenancia C, Vaz-Luis I, Di Meglio A, Pistilli B, Coutant C, Cottu P, Lesur A, Petit T, Dalenc F, et al. Association of body mass index and cardiotoxicity related to anthracyclines and trastuzumab in early breast cancer: French CANTO cohort study. *PLoS Med.* 2019;16:e1002989. doi: 10.1371/journal.pmed.1002989

24. Jeyaprakash P, Sangha S, Ellenberger K, Sivapathan S, Pathan F, Negishi K. Cardiotoxic effect of modern anthracycline dosing on left ventricular ejection fraction: a systematic review and meta-analysis of placebo arms from randomized controlled trials. *J Am Heart Assoc.* 2021;10:e018802. doi: 10.1161/JAHA.120.018802

25. How O, Aasum E, Kunnathu S, Severson DL, Myhre ESP, Larsen TS. Influence of substrate supply on cardiac efficiency, as measured by pressure-volume analysis in ex vivo mouse hearts. *Am J Physiol Heart Circ Physiol.* 2005;288:H2979–H2985. doi: 10.1152/ajpheart.00084.2005

26. Doenst T, Nguyen TD, Abel ED. Cardiac metabolism in heart failure: implications beyond ATP production. *Circ Res.* 2013;113:709–724. doi: 10.1161/CIRCRESAHA.113.300376

27. Kantor PF, Lucien A, Kozak R, Lopaschuk GD. The antianginal drug trimetazidine shifts cardiac energy metabolism from fatty acid oxidation to glucose oxidation by inhibiting mitochondrial long-chain 3-ketoacyl coenzyme A thiolase. *Circ Res.* 2000;86:580–588. doi: 10.1161/01.res.86.5.580

28. Santos-Gallego CG, Requena-Ibanez JA, San Antonio R, Ishikawa K, Watanabe S, Picatoste B, Flores E, Garcia-Ropero A, Sanz J, Hajjar RJ, et al. Empagliflozin ameliorates adverse left ventricular remodeling in nondiabetic heart failure by enhancing myocardial energetics. *J Am Coll Cardiol.* 2019;73:1931–1944. doi: 10.1016/j.jacc.2019.01.056

29. Santos-Gallego CG, Requena-Ibanez JA, San Antonio R, Ishikawa K, Watanabe S, Picatoste B, Flores E, Garcia-Ropero A, Sanz J, Hajjar RJ, et al. Empagliflozin ameliorates adverse left ventricular remodeling in nondiabetic heart failure by enhancing myocardial energetics. *J Am Coll Cardiol.* 2019;73:1931–1944. doi: 10.1016/j.jacc.2019.01.056

30. Kirkham AA, Pituskin E, Mackey JR, Grenier JG, Ian Paterson D, Haykowsky MJ, Thompson RB. Longitudinal changes in skeletal muscle metabolism, oxygen uptake, and myosteatosis during cardiotoxic treatment for early-stage breast cancer. *Oncologist.* 2022;27:e748–e754. doi: 10.1093/oncolo/oyac092

31. Chance B, Leigh JSJ, Clark BJ, Maris J, Kent J, Nioka S, Smith D. Control of oxidative metabolism and oxygen delivery in human skeletal muscle: a steady-state analysis of the work/energy cost transfer function. *Proc Natl Acad Sci U S A.* 1985;82:8384–8388. doi: 10.1073/pnas.82.24.8384

32. Shachar SS, Williams GR, Muss HB, Nishijima TF. Prognostic value of sarcopenia in adults with solid tumours: a meta-analysis and systematic review. *Eur J Cancer.* 2016;57:58–67. doi: 10.1016/j.ejca.2015.12.030

33. Anjanappa M, Corden M, Green A, Roberts D, Hoskin P, McWilliam A, Choudhury A. Sarcopenia in cancer: risking more than muscle loss. *Tech Innov Patient Support Radiat Oncol.* 2020;16:50–57. doi: 10.1016/j.tipsro.2020.10.001

34. Wisdom KM, Delp SL, Kuhl E. Use it or lose it: multiscale skeletal muscle adaptation to mechanical stimuli. *Biomech Model Mechanobiol.* 2015;14:195–215. doi: 10.1007/s10237-014-0607-3

35. Clark BC. Neuromuscular changes with aging and sarcopenia. *J Frailty Aging.* 2019;8:7–9. doi: 10.14283/jfa.2018.35

36. Abete I, Konieczna J, Zulet MA, Galmés-Panades AM, Ibero-Baraibar I, Babio N, Estruch R, Vidal J, Toledo E, Razquin C, et al; PREDIMED-PLUS Investigators. Association of lifestyle factors and inflammation with sarcopenic obesity: data from the PREDIMED-Plus trial. *J Cachexia Sarcopenia Muscle.* 2019;10:974–984. doi: 10.1002/jcsm.12442

37. Wooten SV, Roth M, Livingston JA, Hildebrandt MAT, Chandra J, Amini B, Kleinerman ES, Gilchrist SC. Short-term changes in skeletal muscle mass after anthracycline administration in adolescent and young adult sarcoma patients. *J Adolesc Young Adult Oncol.* 2022;11:320–322. doi: 10.1089/jayao.2021.0107

38. Tarpey MD, Amorese AJ, Balestrieri NP, Fisher-Wellman KH, Spangenburg EE. Doxorubicin causes lesions in the electro7n transport system of skeletal muscle mitochondria that are associated with a loss of contractile function. *J Biol Chem.* 2019;294:19709–19722. doi: 10.1074/jbc.RA119.008426

39. Tajsharghi H, Oldfors A. Myosinopathies: pathology and mechanisms. *Acta Neuropathol.* 2013;125:3–18. doi: 10.1007/s00401-012-1024-2

40. Gilliam LAA, St Clair DK. Chemotherapy-induced weakness and fatigue in skeletal muscle: the role of oxidative stress. *Antioxid Redox Signal.* 2011;15:2543–2563. doi: 10.1089/ars.2011.3965

41. Foulkes SJ, Howden EJ, Haykowsky MJ, Antill Y, Salim A, Nightingale SS, Loi S, Claus P, Janssens K, Mitchell AM, et al. Exercise for the prevention of anthracycline-induced functional disability and cardiac dysfunction: the BREXIT study. *Circulation.* 2023;147:532–545. doi: 10.1161/CIRCULATIONAHA.122.062814

42. Vanhamme L, van den Boogaart A, Van Huffel S. Improved method for accurate and efficient quantification 7of MRS data with use of prior knowledge. *J Magn Reson.* 1997;129:35–43. doi: 10.1006/jmre.1997.1244

43. Buerger C, Sénégas J, Kabus S, Carolus H, Schulz H, Agarwal H, Turkbey B, Choyke PL, Renisch S. Comparing nonrigid registration techniques for motion corrected MR prostate diffusion imaging. *Med Phys.* 2015;42:69–80. doi: 10.1118/1.4903262